Available at www.ijcasonline.com ISSN:2349 – 0594

International Journal of Modern Chemistry and Applied Science

International Journal of Modern Chemistry and Applied Science, 2016, 3(4), 469-472

Plant Mediated Synthesis of Silver Nanoparticles Using Mimosa Mucilage Gum: Characterization, Antibacterial and Catalytic Activity

Bhagavanth Reddy G [a], N Chandra Shakar Reddy [b] and Kotu Girija Mangatayaru [c]*

[a]*Department of Chemistry, PG Centre Wanaparthy, Palamuru University, Mahabub nagar, TS, India.*
[b] *Department of Zoology, PG Centre Wanaparthy, Palamuru University, Mahabub nagar, TS, India.*
[c] *Department of Chemistry, Palamuru University, Mahabub nagar, TS, India.*
Mailing. kotugirija@rediffmail.com

Abstract: Here, we report synthesis, characterization, anti-bacterial activity and catalytic evaluation of silver nanoparticles (AgNPs) using Mimosa Mucilage Gum (MM gum), acting as both reducing and stabilizing agent without using any toxic reagents. The AgNPs were synthesized using hydrothermal method in an autoclave. The synthesized AgNPs were characterized byUV–Visible spectroscopy (UV-Vis), X-ray diffraction (XRD), Fourier transform infrared spectroscopy (FTIR) and Transmission electron microscopy (TEM). The catalytic activity of AgNPs was evaluated on the reduction of Hexacyanoferrate (III) and $NaBH_4$ using spectrophotometry. The MM gum capped silver nanoparticles showed significant antibacterial action on both the gram classes of bacteria.

Key words: Silver nanoparticles, MM gum, green synthesis, catalytic activity, antibacterial activity.

1.Introduction

Metal nanoparticles show vital role in science and technology due to their shape and unique size dependent properties which makes useful in variety of applications including electronic devices, catalysts, chemical /optical sensors, drug delivery and antibacterial activity[1-8].Widespread synthesis protocols used for AgNPs production require the use of strong reducing agents (hydrazine or borohydride) and harsh organic surfactants/ solvents, were naturallyproduce large quantities of hazardous waste [9-15]. Hence, the AgNPs synthesis procedures that eliminate the usageof hazardous reagents, cost-effective and afford greener substitutions are muchneeded as the number of nanoparticle applications increases.

The replacement of non-ecofriendly synthesis methods with non-toxic and clean green chemistry methods is the present need in the production of AgNPs. Several biological systems such as fungi, fruit extract, bacteria and plants can actively reduce metal ions to form metal nanoparticles in an ecofriendly manner. Among these, natural gums obtained from plants such as gum karaya, gum acacia, gum kondagogu and katira gum, (natural polymers), etc., act as reducing agents and capping agents [16-17].Mimosa Mucilage Gum is found from seeds of Mimosa pudica(family:Mimosaceae). Seed mucilage is composed of D-glucuronic acid and D-xylose. Mimosa seed mucilage hydrates and swells rapidly when contact with water. Hence, MM gum was used in drug delivery [18].

Antimicrobial agents are significantarms in fighting bacterial infections and have significance in the health-related quality of human life. Organic compounds used as disinfectantshave disadvantages, including toxicity to the humanbody. For that reason, the interest in inorganic disinfectantssuch as metal nanoparticles (NPs) is increasing. In addition, AgNPs with smaller particle size were reportedto show good antimicrobial activity. Metal nanoparticles can act as a good catalyst due to the high Fermi potential. AgNPs can catalyze many reduction reactions [16,17].

In this investigation, we report a facile, simple and fast method for the synthesis of AgNPs using a natural polymer MM gum (without any additional reducing and stabilizing agents) as the synthesized nanoparticles were characterized by using UV-Vis, FTIR, XRD and TEM and the green synthesized AgNPs were showed good catalytic and anti-bacterial activities.

Experimental section

2.1 Materials

Silver nitrate ($AgNO_3$, 99.9%) was purchased from sigma Aldrich, and sodium borohydride ($NaBH_4$, 98%), nitric acid (HNO_3), hydrochloric acid (HCl) and [$K_3(FeCN)_6$] were purchased from S-D Fine chemicals. MM gum was purchased from Girijan Co-operative Corporation Limited.

2.2 Method

All the solutions were prepared in Milli-Q water. 0.5 % (w/v) of homogeneous gum stock solution was prepared by adding a calculated quantity of MM gum powder into the reagent bottle containing milli-q water and stirring the same for 1 h at room temperature. 0.5 % of 1 mL $AgNO_3$solution and 3 mL of MM gum solution were mixed in a boiling tube. This mixture was kept in an autoclave at 30 psi pressure and 120 ^oC for 30 min [16].

Catalytic reduction of hexacyanoferrate (III)

Electron Transfer Reaction occurs between Hexacyanoferrate (III) and $NaBH_4$. A reaction mixture containing 1.0 mL of double-distilled water, 0.6 mL of $K_3Fe(CN)_6$ aqueous solution (10 mM), and 1.4 mL of $NaBH_4$(36 mM) in 0.1 M NaOH aqueous solution were taken in a 3 mL quartz cuvette. Then, the AgNPs were added to this reaction mixture. The alkaline solution could minimize the decomposition of borohydride. The reduction was monitored at 420 nm by using an UV-visible spectrophotometer [17].

Antibacterial property

Antibacterial properties of the synthesized AgNPs were carried out using the disc diffusion method. Gram-

positive and Gram-negative bacteria, Staphylococcus aureus and Pseudomonas putida respectively, were used as model test strains. Luria–Bertani (LB) agar medium was prepared and transferred to sterilized petri dishes. The medium was allowed to solidify and then the petri plates were spread with both bacteria separately in a laminar air flow hood. Using micropipette, 5 and 10 µL of the AgNPs solution and 5 µL of MM gum solutions were added to each well on both plates. The discs were air dried in laminar hood and incubated at 37^0C for 24 h. Then, the zone of inhibition of bacteria was measured. The assays were performed in triplicate [16].

Characterization techniques

The resulting MM gum capped AgNPs solution was analysed by UV–Vis absorption spectrophotometer (Model: Shimadzu UV–Vis 3600, Shimadzu Corporation, Japan) in the range of 200–700 nm. FTIR analysis was carried out on the aqueous solution of synthesized AgNPs using FTIR Spectrophotometer (Model: IRAffinity-1, Shimadzu Corporation, Japan) in the scanning range of 650–4000 cm -1. XRD analysis was conducted on a Rigaku-Miniflex method with Cuka radiation. TEM analysis was performed using a transmission electron microscope (Model: 1200EX, JEOL Ltd., Japan).

4. Results and Discussion:

4.1 UV-Visible spectroscopy

The UV–Vis spectroscopy is one of the most significant technique for determining the formation as well as size of the metal nanoparticles [16]. UV–Vis spectra of the AgNPs are shown in Figure.1.The absorbance maximum was observed in the range of 410–425 nm, which is characteristic of silver surface plasmon resonance. To optimize the synthesis of nanoparticles, the influence of parameters such as concentration of gum and concentration of $AgNO_3$ was studied. Figure.1 shows the UV–Vis spectra of the synthesized AgNPs with different concentrations of MM gum (0.1–0.5 %) with 0.5% $AgNO_3$ and 30 min of autoclaving time. Figure.1 shows that it reveals that the formation of nanoparticles increases with increasing concentration of gum. Figure.2shows the UV–Vis spectra of the synthesized AgNPs at different concentrations of $AgNO_3$ (0.1–0.5%) containing 0.5 % of gum with an autoclaving time of 30 min which indicates that the formation of nanoparticles increases with increase in the concentration of $AgNO_3$.

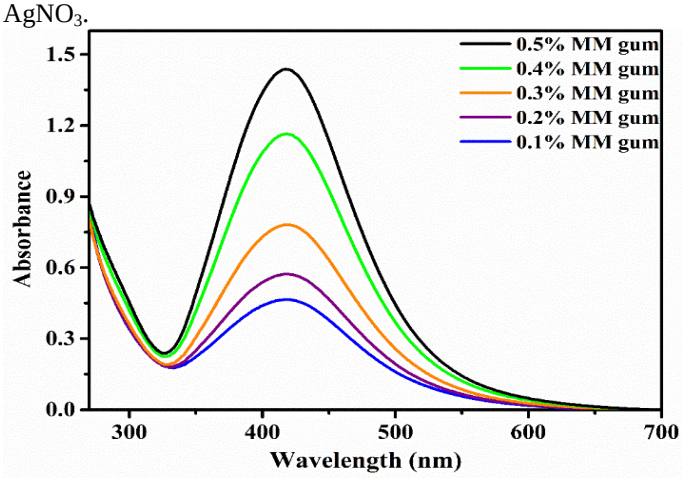

Figure.1. The UV–Vis absorption spectra of AgNPs synthesized by autoclaving different concentrations of MM gum solution with 0.5% $AgNO_3$.

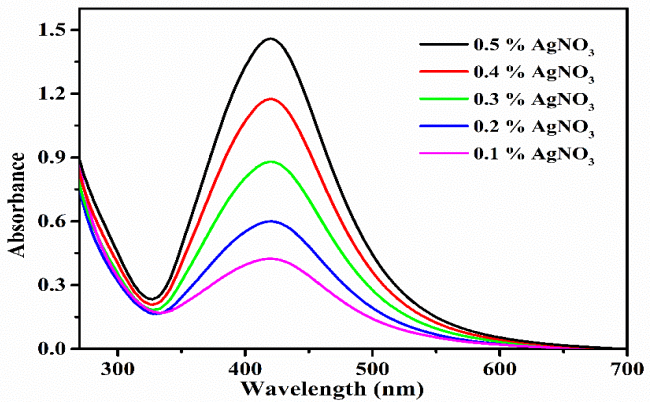

Figure.2. The UV–Vis absorption spectra of AgNPs synthesized by autoclaving different concentrations of $AgNO_3$ with 0.5 % MM gum solution.

FTIR

The identification of the possible functional groups involved in the reduction and the stabilization of AgNPs can be evaluated by the FTIR spectroscopy. The major frequencies that are found in the FTIR spectrum of MM gum are 3358, 2937, 2347, 1719, 1593, 1367,1254 and 1017 cm-1(Figure.3 curve (a)). The broad band peakobserved at 3358 cm^{-1}could be assigned to stretchingvibrations of –OH groups in MM gum. The bands at 2937cm^{-1} correspond to asymmetric stretching vibrations of methylene group. The broad band at 1719 cm^{-1} could beassigned to carbonyl stretching vibrations in ketones,aldehydes and carboxylic acids. The sharp band found at1593 cm^{-1}could be assigned to characteristic asymmetrical stretch of carboxylate group. The band foundat 1367 cm^{-1}could be assigned to characteristic bendingof –C–H group. The peak at 1254 $cm^{-1}$was due to the C–O stretching vibrations of polyols and alcoholic groups. While the IR spectrum of MM gum capped AgNPs showed(Figure.3curve b) characteristic absorbance bands at 3427, 2927,2350, 1731, 1605, 1424, 1255 and 1029 cm^{-1},respectively, in the IR spectrum of nanoparticles, a shift inthe absorbance peaks was observed from 3358 to 3427,1719–1731, 1593–1605 and 1367–1424 cm^{-1}. FTIRspectral studies suggest that the carbonyl and hydroxylgroups have a stronger affinity to bind with metal andfacilitate the formation of a coat over the nanoparticles andfavour in stabilizing the AgNPs against agglomeration.

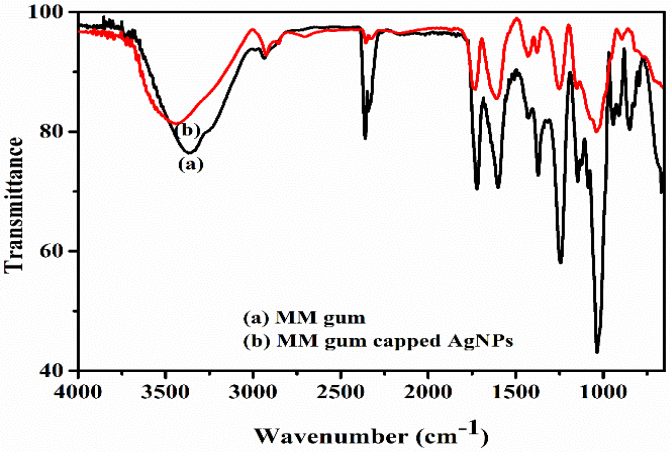

Figure.3 FTIR spectra of (a) MM gum, (b) AgNPs stabilized in bhara gum.

XRD

To further confirm the formation of silver nanoparticles by powder XRD pattern. Diffraction peaks were detected at 2θ 38.03, 44.13, 64.24 and 77.31 (Figure.4) which can be indexed as (111), (200), (220) and (311), respectively, and the planes of face-centred cubic (fcc) AgNPs. The existence of diffraction peaks were matched to the standard data files (the JCPDS card No. 04-0784) for all reflections. The XRD pattern shows that synthesized silver nanoparticles are purely crystalline nature.

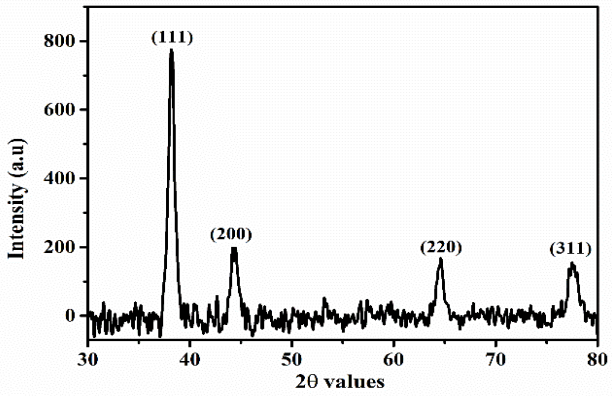

Figure. 4. XRD pattern of synthesized silver nanoparticles.

TEM

The size, morphology and shape of the green synthesized AgNPs were elucidated with the help of TEM. Figure. 5 shows the TEM images of the silver nanoparticles synthesized. These TEM images it is observed that though, the nanoparticles are predominantly spherical. The average particle size obtained from these micrographs was about 12±4 nm. Figure.6 shows the corresponding size distribution histogram of the nanoparticles. The particle size is distributed in the range of 4-29 nm and average particle size is 12 ± 4 nm.

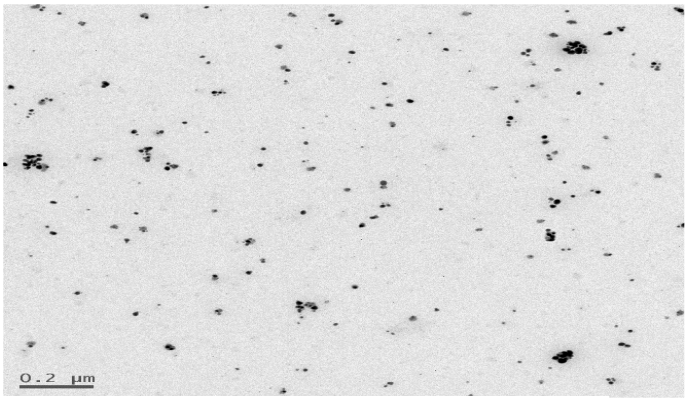

Figure.5 TEM image of synthesized silver nanoparticles.

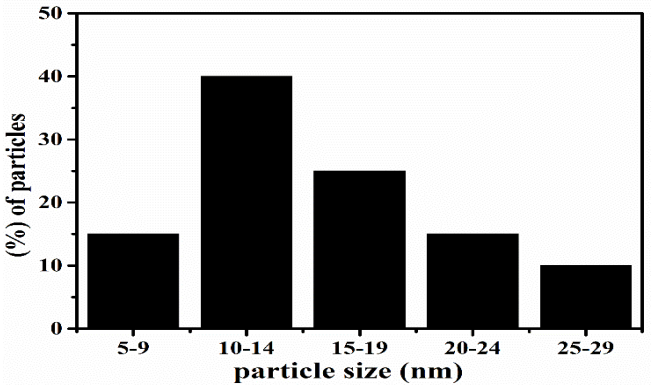

Figure.6. Histogram of synthesized silver nanoparticle.

Catalytic Reduction of hexacyanoferrate (III)

Electron transfer reaction that has been used as a model reaction to study catalysis by silver nanoparticles is the reduction of hexacyanoferrate (III) by borohydride ions. This is an interesting reaction because both oxidation states in iron (+2 and +3) are stable with respect to hydrolysis and dissociation and possess the same chemical composition and geometry. This reaction in aqueous solution can be written.

$$BH_4^- + 8[Fe(CN)_6]^{3-} + 3H_2O \rightarrow H_2BO_3^- + 8[Fe(CN)_6]^{4-} + 8H^+ \quad (1)$$

The reaction can even proceed without a catalyst, but it has been reported that it is a slow reaction, which follows zero-order kinetics [17]. Interestingly, MM gum stabilized silver nanoparticles can be efficiently used as catalysts for this electrochemical reaction. It has been shown that MM gum containing functional groups adsorbed on the surface of the silver nanoparticles provide sufficient surface charge to prevent nanoparticle aggregation. In fact, related electron injection processes were reported in the past for gold colloids, which demonstrated this ability of nanoparticles to function as nano electrodes [17]. Thus, once the nanoparticle surface is charged by the addition of a reducing agent, the stored electrons can be discharged if an electron acceptor is introduced into the system.

In the presence of noble metal nanoparticles, the catalysis mechanism involves a two-step process as shown in eqs. (2) and eqs (3)

$$BH_4^- + \text{Metal} \leftrightarrow Q^- \text{(fast)} \quad (2)$$

$$Q^- + [Fe(CN)_6]^{3-} \rightarrow [Fe(CN)_6]^{4-} + Q \text{ (slow)} \quad (3)$$

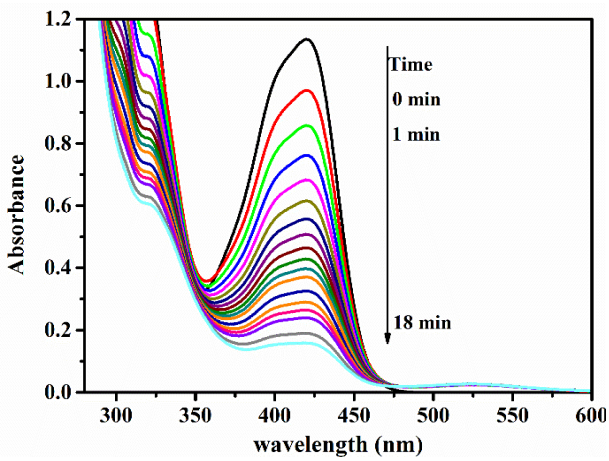

Figure. 7. Time dependent UV-vis spectra of the mixture of hexacyanoferrate (III) and sodium borohydride upon addition of silver nanoparticles.

In an initial step, borohydride can inject electrons onto silver nanoparticles. The reaction is completed in a second, slow step whereby ferricyanide ions diffuse to the nanoparticle surface and are reduced by excess surface electrons. It should be noted that the non catalyzed reaction of eq. (1) can be neglected since it is much slower than the catalyzed reaction of eqs. (2) and (3). In the experimental runs, the concentration of $NaBH_4$ was set to in large excess as compared to hexacyanoferrate (III) ions. Thus, the kinetics of the reduction process can be regarded as a pseudo-first-order reaction. The progression of the reaction was

monitored indirectly through the UV-Vis spectrum of hexacyanoferrate (III). The characteristic absorption peak of hexacyanoferrate (III) is located at 420 nm, and its intensity was continuously decreased immediately after the addition of silver nanoparticles, revealing the occurrence of catalyzed reduction. As seen in Figure 8, the UV-Vis spectra were recorded and the absorption peak of hexacyanoferrate (III) decreased quickly and completely disappeared. The rate constant (k) was calculated from the linear plot of ln (A_0/A_t) versus reduction time, in Fugure.8 the rate constant was found k = 0.098 min^{-1}

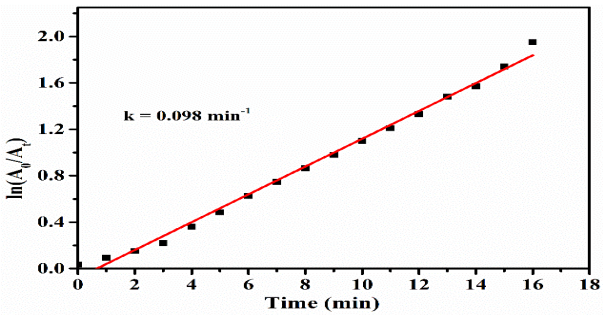

Figure. 8. The plot of ln (A_0/A_t) versus time for the reduction of Fe^{+3} to Fe^{+2}.

Antibacterial activity

Antibacterial activity of green synthesized gold nanoparticles against Gram negative Pseudomonas putida (P. putida) and Gram positive Staphylococcus aureus (S. aureus), [16] bacteria at different concentrations showed that they revealed a strong dose-dependent antibacterial activity against the test microorganisms. It was seen that, as the concentration of green synthesized silver nanoparticles were increased, bacterial growth decreases in both the cases. The zone of inhibition of silver nanoparticles against Gram positive and Gram negative bacteria shown in (Figure.6A, 6B). The results indicated that silver nanoparticles synthesized from MM gum showed effective antibacterial activity in Gram positive than in Gram negative bacteria respectively. No zone of inhibition was observed for the gum alone. Based on these results, it can be concluded that the synthesized silver nano particles had significant antibacterial action on both the Gram classes of bacteria.

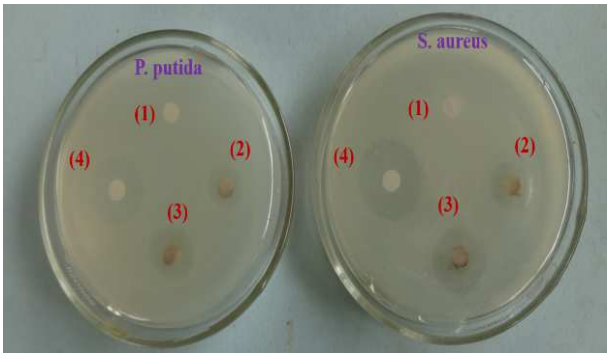

Figure. 9Antibacterial activity of AgNPs against S. aureus and P. putida after 24 h of incubation.1) 10 µL of pure MM gum solution,2)5 µL of AgNPs,3) 10 µL of AgNPs, 4) 5 µL of ampicillin.

4. Conclusion

MM gum is an efficient source for the synthesis of AgNPs. The synthesized AgNPs were characterized by various techniques. The XRD pattern showed that the synthesized AgNPs were essentially crystalline. In FTIR analysis, it is foundthat both hydroxyl and carbonyl groups of MM gum are involved in the synthesis and stabilization of AgNPs. The size and shape by TEM showed that the synthesized AgNPs were spherical in shape and crystalline in naturewith the average size distribution of 12±2 nm. The catalytic activity of green synthesized AgNPs was examined byelectron transfer reaction between hexacyanoferrate (III) and sodium borohydride, resulting in the formation of hexacyanoferrate (II) ions and dihydrogen borate ions. The synthesized AgNPs showed significantantibacterial action on both the gram classes of bacteria. Hence, we conclude that the green synthesized AgNPs were showed good catalytic and anti-bacterial activities.

5. References

1. V. H. Grassian; Journal of Physical Chemistry C, 112, 18303–18313, 2008.
2. P. K. Jain, K. S. Lee, I. H. El-Sayed, and M. A. El-Sayed; Journal of Physical Chemistry B,110, 7238–7248, 2006.
3. C. Liu and Z. J. Zhang; Chemistry of Materials, 13, 2092–2096, 2001.
4. X.H.N.Xu, S. Huang, W. Brownlow, K.Salaita, and R. B. Jeffers; Journal of Physical Chemistry B,108,15543–15551, 2004.
5. D. Manno, E. Filippo, M. Di Giulio, and A. Serra; Journal of Non-Crystalline Solids, 354, 5515–5520, 2008.
6. Y. J. Kim, Y. S. Yang, S. -C. Ha; Sensors and Actuators B, 13,189–198, 2005.
7. A. Prakash, J. Ouyang, J. L. Lin, and Y. Yang; Journal of Applied Physics, 100, 054309, 2006.
8. A. D. LaLonde, M. G. Norton, D. Zhang; Journal of Materials Research, 20, 3021–3027, 2005.
9. M. Brust, M.Walker, D. Bethell, D. J. Schiffrin, and R. Whyman; Journal of the Chemical Society, Chemical Communications, 7, 801–802, 1994.
10. A. P.Herrera, O. Resto, J. G. Briano, and C. Rinaldi; Nanotechnology, 16, S618–S625, 2005.
11. C. L. Kitchens,M.C.McLeod, andC.B.Roberts; Langmuir, 21, 5166–5173, 2005.
12. M.-L. Wu and L.-B. Lai; Colloids and Surfaces A, 244, 1–3,149–157, 2004.
13. J. Liu, J. Sutton, and C. B.Roberts; Journal of Physical Chemistry C, 111, 11566– 11576, 2007.
14. J. Liu, M. Anand, and C. B. Roberts; Langmuir, 22, 3964–3971, 2006.
15. J. Liu, F. He, T. M. Gunn, D. Zhao, and C. B. Roberts; Langmuir, 25, 7116–7128, 2009.
16. G. Bhagavanth Reddy, A. Madhusudhan, D. Ramakrishna and G. Veerabhadram; J Nanostruct Chem, DOI 10.1007/s40097-015-0149-y.
17. G. Bhagavanth Reddy, A. Madhusudhan, D. Ramakrishna and G. Veerabhadram; J. Chin. Chem. Soc, 62,420-428, 2015
18. K. Singh, A. Kumar, N. Langyan, and M. Ahuja; AAPS PharmSciTech, 10, 1121–1127, 2009.